Computer Methods in Biomechanics and Biomedical Engineering,
Vol. 11, No. 1, February 2008, 41–53

Taylor & Francis
Taylor & Francis Group

Integrating modelling, motion capture and x-ray fluoroscopy to investigate patellofemoral function during dynamic activity

J. W. FERNANDEZ†*, M. AKBARSHAHI†, H. J. KIM† and M. G. PANDY†‡

†Department of Mechanical and Manufacturing Engineering, University of Melbourne, Melbourne 3010, Vic., Australia
‡Department of Biomedical Engineering, University of Texas at Austin, 1 University Station, C0800, Austin, TX 78712-0238, USA

Accurate measurement of knee-joint kinematics is critical for understanding the biomechanical function of the knee *in vivo*. Measurements of the relative movements of the bones at the knee are often used in inverse dynamics analyses to estimate the net muscle torques exerted about the joint, and as inputs to finite-element models to accurately assess joint contact. The fine joint translations that contribute to patterns of joint stress are impossible to measure accurately using traditional video-based motion capture techniques. Sub-millimetre changes in joint translation can mean the difference between contact and no contact of the cartilage tissue, leading to incorrect predictions of joint loading. This paper describes the use of low-dose X-ray fluoroscopy, an *in vivo* dynamic imaging modality that is finding increasing application in human joint motion measurement. Specifically, we describe a framework that integrates traditional motion capture, X-ray fluoroscopy and anatomically-based finite-element modelling for the purpose of assessing joint function during dynamic activity. We illustrate our methodology by applying it to study patellofemoral joint function, wherein the relative movements of the patella are predicted and the corresponding joint-contact stresses are calculated for a step-up task.

Keywords: Finite-element modelling; Motion capture; Fluoroscopy; Patella; Contact mechanics

1. Introduction

Numerous techniques are available for measuring the kinematics of human movement, including stereophotogrammetry; electromagnetic tracking; imaging modalities, such as magnetic resonance imaging (MRI) and computed tomography (CT); direct invasive techniques, such as implanted bone pins; and *in vitro* methods using cadaver specimens and dry bones.

Stereophotogrammetry or marker-based movement analysis is the most commonly used method for quantitative assessment of joint movement. A combination of data recorded using force plates, skin-mounted reflective markers and video cameras facilitates non-invasive 3D measurement of joint kinematics and kinetics. The errors with skin-mounted markers are well-known and are highlighted in figure 1, where a marker on the femoral epicondyle that is used to locate the flexion-extension axis of the knee shifts anteriorly by a few centimetres as the knee extends during a weight-bearing manoeuvre. Similar errors for a range of tasks have been reported for skin-based marker systems when compared to fluoroscopy (Stagni *et al.* 2005) and bone-pin markers (Fuller *et al.* 1997). Point cluster techniques and optimisation have been used to reduce skin movement artefact. In this approach, the redundant markers are weighted with respect to the placement site and the expected deformation relative to the underlying bony structure (Andriacchi *et al.* 1998). Other methods for reducing errors due to skin movement artefact include the double-calibration technique (Cappello *et al.* 2005), in which the positions of the markers in full joint flexion and full joint extension are captured, and a linear deformation of the body between the two poses is then used to correct for the errors due to skin motion. Validation studies using 3D fluoroscopy on the knee have shown that, the double-calibration technique is accurate to 2.8 mm in translation and 1.6° in rotation. A general disadvantage of using redundant markers is that, they can alter the normal walking pattern of subjects. Apart from the errors introduced by skin movement artefact, errors associated with inter- and intra-trial inconsistency in placing markers relative to internal bony landmarks are also possible.

*Corresponding author. Email: justinf@unimelb.edu.au

Computer Methods in Biomechanics and Biomedical Engineering
ISSN 1025-5842 print/ISSN 1476-8259 online
http://www.tandf.co.uk/journals
DOI: 10.1080/10255840701551046

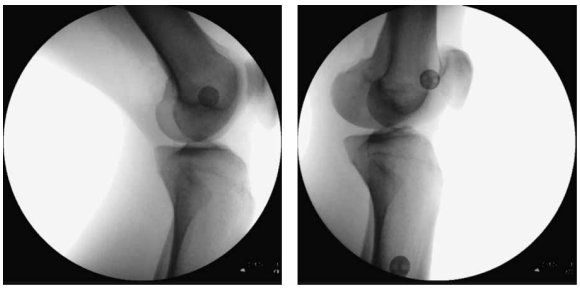

Figure 1. Knee marker tracking the location of the lateral epicondyle on the femur during weight-bearing knee flexion/extension. The image in the right panel shows how the marker shifts anteriorly relative to the femoral epicondyle as the knee extends.

Magnetic tracking methods have also been trialed, where measurement studies using external sensors fixed to a body segment, recorded the changing position and orientation of the segment in time. Problems with this approach include skin movement artefact, sensitivity of the system to magnetic components such as implants, and a limited measuring volume. Nonetheless, magnetic tracking methods have been used to measure carpal (Ishikawa *et al.* 1997) and patellofemoral (Laprade and Lee 2005) kinematics *in vivo*. The inherent accuracy of magnetic systems in an ideal environment is between 0.2 and 0.9 mm in translation and 0.1 – 1° in rotation (Luo *et al.* 1996, Milne *et al.* 1996).

Marker-less methods not only eliminate the need for external markers and the problems associated with skin motion artefact, they also reduce preparation time. An example of this approach is a template using a spandex suit, which is then used to fit subject motion during locomotion (Alexander and Andriacchi 2003). Some studies, have compared motion measurement accuracy using marker-less and marker-based methods and have shown good correlation between the results obtained for the sagittal and frontal planes during gait (Mundermann *et al.* 2006). Marker-less recording has applications in surveillance, animation and virtual reality, but the potential of the method to measure small changes in joint displacement values is questionable.

X-ray methods, such as CT, can provide accurate measurements of bone poses *in vivo*, but for dynamic activity the radiation dose is not justifiable for a healthy subject. Typically, CT is used to obtain detailed bone geometry from a single static orientation and is suitable for threshold segmentation methods (Mahfouz *et al.* 2005). Unfortunately, CT does not provide information about cartilage, muscle attachment sites and other soft tissue geometry, which is required for joint contact problems. By comparison, MRI provides a useful means of obtaining estimates of cartilage volume, muscle attachment locations and bone boundaries simultaneously. Although, MR is an expensive imaging modality, recent advances have enabled quasi-static (Patel *et al.* 2003) and dynamic (Sheehan *et al.* 1999, Asakawa *et al.* 2003) activities to be studied *in vivo*. Further improvements include, open- and weight-bearing MRI (Besier *et al.* 2005), which have been used to study tasks, such as squatting. Another sequence that is becoming more common is called Cine Phase MRI, which, by recording velocity information, allows the position of a single particle to be tracked throughout the images. The main disadvantage of this method is that, it requires the subject to perform repetitive tasks, which can lead to fatigue and changed movement patterns (Sheehan *et al.* 1999). Real-time MRI has addressed some of the afore-mentioned problems, including cyclic repetition of the task. This imaging technique, acquires the anatomy and velocity vectors of the muscle tissues in one dynamic motion. The method is, therefore, quick and offers a higher accuracy in terms of velocity measurements. Its applicability, however, is limited to slow movements (Asakawa *et al.* 2003). In general, the bone segmentation is at best semi-automated, time-consuming and requires much user intervention. Implants can also be a problem and must be checked for compatibility with the MRI strength; 1.5 or 3 T (Shellock and Crues 2004).

Radiostereometric analysis (RSA) is very similar to marker-based motion capture analysis, where retro-reflective markers are replaced by radio-opaque markers, and the camera system is replaced by an X-ray system. Sufficient radio-opaque markers are affixed to the bone to define its position and orientation (Valstar 2001, Yuan *et al.* 2002). Conventional, static RSA has had accuracies in the range $\pm 10-250\,\mu$m reported for bi-plane measurement (Karrholm 1989), and 0.9 mm in translation and 0.27° in rotation reported for single-plane measurement (Yuan *et al.* 2002). High-speed, dynamic, bi-planar radiography has been used to study, tibiofemoral kinematics in a canine model with translational and rotational accuracies of 0.064 mm and 0.31° respectively, for walking on a treadmill (Scott Tashman 2003). The main drawback of RSA is that it is invasive, with radiation doses too high for healthy subjects.

X-ray fluoroscopy offers a new approach for obtaining accurate measurement of human joint kinematics. In this method, a pulsed fluoroscopy sequence is coupled to a feedback loop in the camera, which allows the current and voltage to be adjusted, so that optimal image clarity can be obtained with minimal radiation exposure. Fluoroscopy has been reported to have sub-millimetre accuracy for translation and to be within 1° for rotation for the in-plane (image-plane) direction (Fregly *et al.* 2005a). Out-of plane (perpendicular to the image-plane) measurements errors are slightly larger, but bi-plane fluoroscopy has been shown to improve this accuracy (Fregly *et al.* 2005a). The 2D images obtained from fluoroscopy lead to 3D kinematics through a number of different pose estimation methods, such as feature-based (Banks and Hodge 1996, Zuffi *et al.* 1999, Yamazaki *et al.* 2005) and intensity-based methods (Penney *et al.* 1998, You *et al.* 2001, Dennis *et al.* 2005).

While numerous studies have applied fluoroscopic imaging techniques over the past decade, use of these data to drive detailed FE models of the musculoskeletal system

has been scarce. To date, the main use of X-ray methods appears to be in testing TKR implants (Godest *et al.* 2000, Heegaard *et al.* 2001, Halloran *et al.* 2005). FE modelling can be a powerful analysis tool, provided the boundary conditions and input loading are known accurately. Most researchers have driven FE models using loads and boundary conditions from knee simulators (Godest *et al.* 2002) and *in vitro* experiments (Heegaard *et al.* 1995). A few recent studies, have used kinematic data derived from X-ray fluoroscopy as inputs to joint models. For example, fluoroscopic data have been used to drive an elastic-foundation knee model to predict wear patterns (Fregly *et al.* 2005b), and RSA kinematics have been used as input to an explicit FE model of leg hopping (Beillas *et al.* 2004).

In this paper, we describe a modelling framework that integrates a low-dose dynamic X-ray modality (X-ray fluoroscopy) with traditional gait analysis techniques and an anatomically-based FE model of the human patellofemoral joint. Model estimates of quadriceps muscle loading and accurate measurements of tibiofemoral kinematics obtained from X-ray fluoroscopy are input into an anatomically-based FE model of the human patellofemoral joint to determine patella kinematics and contact mechanics for one subject performing a step-up task. The model calculations are qualitatively validated against *in vitro* and *in vivo* data reported in the literature.

2. Methods

Ethical approval for this study, was obtained from the University of Melbourne Ethics Board and the State of Victoria Radiation Safety Advisory Board, Melbourne, Australia. Experiments were performed on one healthy male subject (age = 26, weight = 65 kg, height = 180 cm). The subject gave informed consent by reading and signing a consent form.

Tibiofemoral kinematics can be determined by integrating X-ray fluoroscopy with advanced 2D/3D image registration methods. This process, which is known as pose-estimation, is performed using either single- or bi-plane fluoroscopy. Specifically, 2D images are captured using an X-ray fluoroscopy system, and a 3D model of the knee joint is created using MRI. The 3D model is then virtually projected to create a synthetic 2D X-ray image. The synthetic 2D image is then aligned to the actual X-ray image by minimising the distance between segmented contour features on the images, and the final pose of the knee joint is determined. The accuracy obtained using single-plane fluoroscopy is suitable for all degrees of freedom, except out-of-plane translations (Banks and Hodge 1996, Hoff *et al.* 1998, Fregly *et al.* 2005a). A bi-plane fluoroscopy system can solve this problem, by using the additional information obtained from the other plane (Taiyo Asano *et al.* 2001, 2003, Li *et al.* 2004).

Figure 2 shows the major steps involved in the pose-estimation procedure. First, MR images of the subject's lower limbs were acquired using a Siemens 3 T MRI machine housed at The Royal Children's Hospital, Melbourne. A T2 fat-suppressed sequence was used, as this particular MR sequence is known to aid the bone and cartilage boundary segmentation process by highlighting the difference between the bone and articular cartilage interface.

Second, bone surface meshes were generated using a commercial image processing software package (3D Doctor, Able Software, MA) that allowed, the edges of the bones to be detected more efficiently using internal thresholding. This process was repeated for the articular cartilage with some manual intervention in areas, where the software failed to detect the boundary. For an experienced user this took about 4 h for both the complete femur and tibia bones including an hour of manual intervention. Approximately, the same amount of time was spent for cartilage segmentation with around 2 h of manual intervention required. The manual intervention enabled the user to remove the deleterious confusion between the bone/cartilage boundaries and the surrounding soft tissue structures, such as the fat layers and surrounding bursa (lubricating fat pads), which sometimes caused problems for the automated edge detection software. Unwanted artefacts were removed, and the mesh smoothed before exporting in a stereolithography (STL) format.

Third, motion and force data were recorded as the subject performed a step-up manoeuvre (step height = 15 cm; step length = 69 cm; step velocity = 0.85 ms^{-1}). Six high-speed video cameras (VICON) were used to track lower limb reflective markers, where the marker-set used was the standard Vicon plug-in gait model, namely (heel, toe, mid thigh, mid shank, lateral ankle malleoli, lateral knee epicondyle, anterior superior iliac spine (ASIS) and sacrum), also known as the "Helen Hayes" marker set.

Two AMTI (Advanced Mechanical Technology, Inc., MA, US) force plates were used to record the three components of the ground-reaction force. The relative positions of the femur and tibia were recorded using a Phillips Pulsera Mobile C Arm fluoroscopy unit with the following settings: 9-inch image intensifier, current 0.5 mA and voltage 60 kV. The total effective dose delivered during the experiment was 0.003 mSv, which is in the range of the permissible dose constraint ($<$ 5 mSv per year) as required by the Australian Radiation Protection and Nuclear Safety Agency (ARPANSA 2005). With the fluoroscope sampling at a rate of 30 Hz, the subject performed a step-up manoeuvre that lasted for approximately 1 s.

Fourth, the 3D bone model generated from MRI was registered to the 2D images using a software package called KneeTrack (Banks 2005). This procedure was comprised of a calibration step, which was needed to account for the distortion of the image intensifier and the determination of internal system parameters, followed by a perspective projection of the 3D bone, that matched the bone surfaces

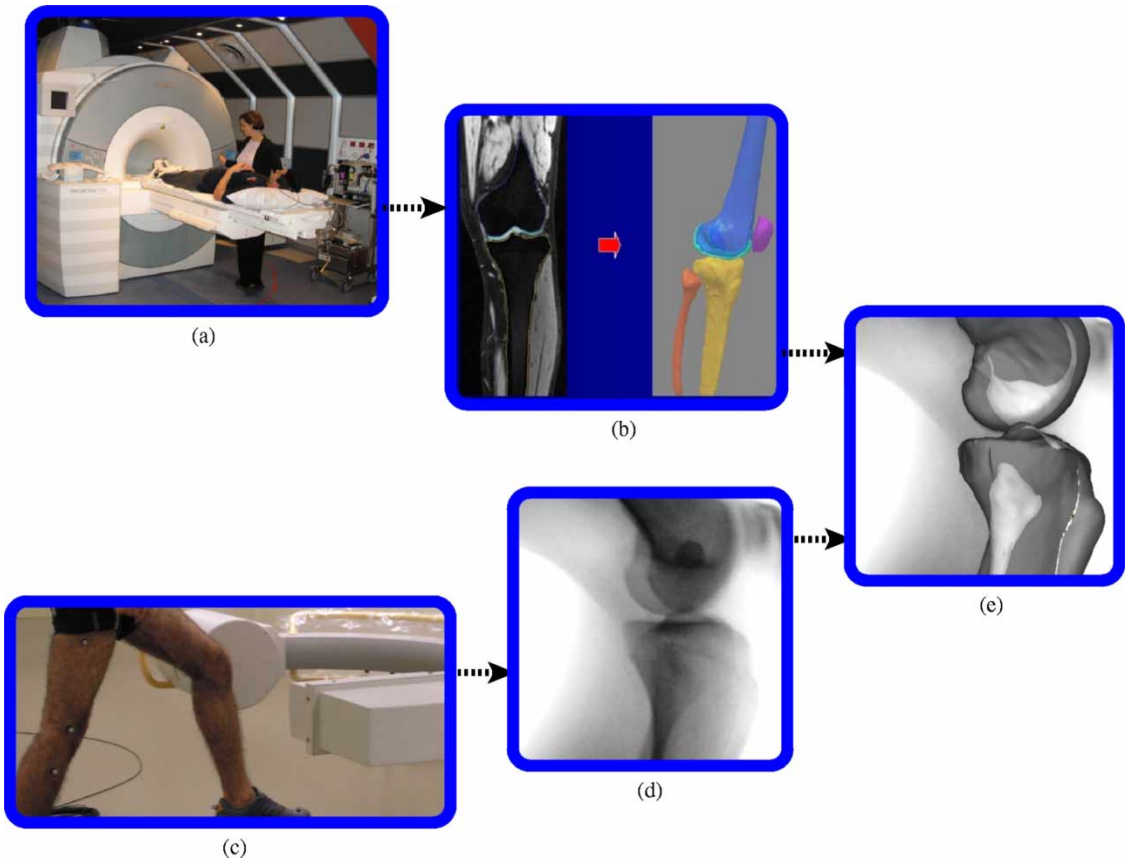

Figure 2. (a) Subject undergoing MRI and (b) geometry segmented to create a 3D computer model of the lower limb. (c) X-ray fluoroscopy capturing dynamic step-up task and (d) resulting 2D video motion. (e) The 3D model was aligned to the 2D video to deduce accurate joint kinematics using the custom software package, KneeTrack (Banks, 2005).

to segmented features on the 2D fluoroscopic image. The bone pose was then optimized to minimize the Euclidean distance between the detected X-ray edge features and the projected bone contours. The optimization problem was solved for all 30 frames captured from the fluoroscopy system and resulted in tibiofemoral kinematics for the step-up task.

We defined the flexion-extension axis of the knee as the line connecting two co-axial cylinders fitted to the medial and lateral condyles of the femur (figure 3). This flexion-extension axis has been shown to represent the actual knee flexion axis for the range 15–115° of knee flexion (Eckhoff *et al.* 2005). To facilitate definition of the coordinate system for the femur, a sphere was also fitted to the femoral head using 3D geometric modelling software called Rhinoceris (McNeel North America, WA, US). The tibial coordinate system was defined using the most medial and lateral points on the tibial plateau together with the ankle joint centre, which is defined using the midpoint between the line connecting the outermost medial edge of distal tibia (medial malleoli) and the outermost lateral edge of the distal fibula (lateral malleoli).

A dry-bone femur-tibia preparation was used to assess the accuracy of the pose-estimation procedure described above. Reflective markers were positioned on the dry bones, and the static positions of the markers were detected by a video-based motion capture system (Vicon, Oxford Metrics Inc.). The marker positions were used to calculate the position and orientation of the tibia relative to the femur in 3D. The image intensifier was calibrated to account for distortion. This was performed by, placing a 1-inch grid of radio-opaque markers (1 mm diameter) against the image intensifier. The X-ray image of this grid was acquired and morphed to the undistorted grid shape using a bilinear vertex transformation (Banks and Hodge 1996). The cadaver bones were then radiated using a pulsed fluoroscopy sequence. Bone geometry and the Vicon markers were then captured using CT to ensure that the same coordinate systems were used, when comparing the results obtained from motion capture and fluoroscopy. Finally, the X-ray image was input to the KneeTrack software to determine the relative positions of the femur and tibia (figure 4).

A musculoskeletal model of the body was used to determine leg-muscle forces during the step-up task. The body was modelled as a 10-segment, 23 degree of freedom articulated linkage actuated by 58 Hill-type musculotendon actuators (Anderson and Pandy 2001a). The pelvis was modelled as a rigid segment with six degrees of freedom. Each hip was modelled as a ball-and-

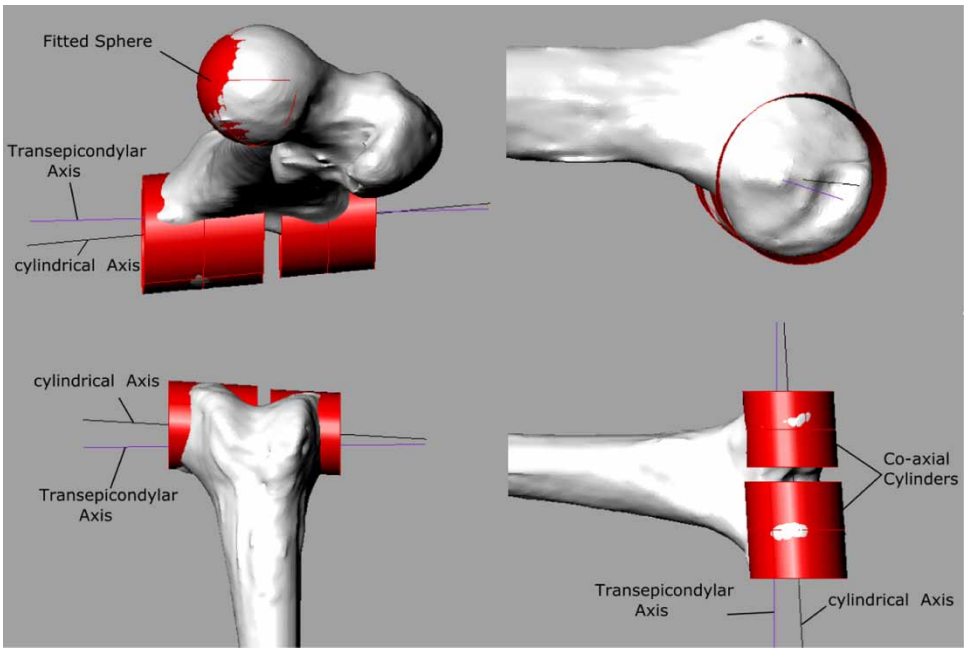

Figure 3. The locations of the joint centres and the position and orientation of the flexion/extension axis of the knee were found by fitting a sphere to the femoral head and cylinders to the femoral condyles.

socket joint, each knee as a hinge joint, each ankle-subtalar joint as a universal joint, and each metatarsal joint as a hinge joint. The head, arms, and torso were represented as a single segment that articulated with the pelvis via a ball-and-socket joint located at approximately the third lumbar vertebra. The inertial properties of the segments were based on the regression equations of McConville *et al.* (1980) and anthropometric measures obtained from five healthy adult males (Anderson and Pandy 2001a). Each muscle tendon actuator was represented as a three-element, Hill-type muscle in series with an elastic tendon (Zajac 1989). The paths of all the muscles, except vasti, hamstrings, and gastrocnemius, were identical to those represented in the model described by Anderson and Pandy (2001a). Whereas, vasti, hamstrings, and gastrocnemius were each represented by a single muscle in the walking model, the separate portions of each of these muscles were included in the present model. Specifically, vasti was represented by the vastus medialis, intermedius, and lateralis; hamstrings by the semitendinosus, semimembraneosus, biceps femoris long head, and biceps femoris short head; and gastrocnemius by its medial and lateral heads. The patellar tendon stiffness and articular cartilage Young's modulus were assumed to be $300\,\mathrm{Nmm}^{-1}$ and 40 MPa, respectively, and the value of Poisson's ratio for cartilage was taken to be 0.45. These values were adapted from a previous FE model of the lower limb developed by Beillas *et al.* (2004). Moreover, a value of 0.45, which assumes that cartilage is nearly incompressible is a reasonable

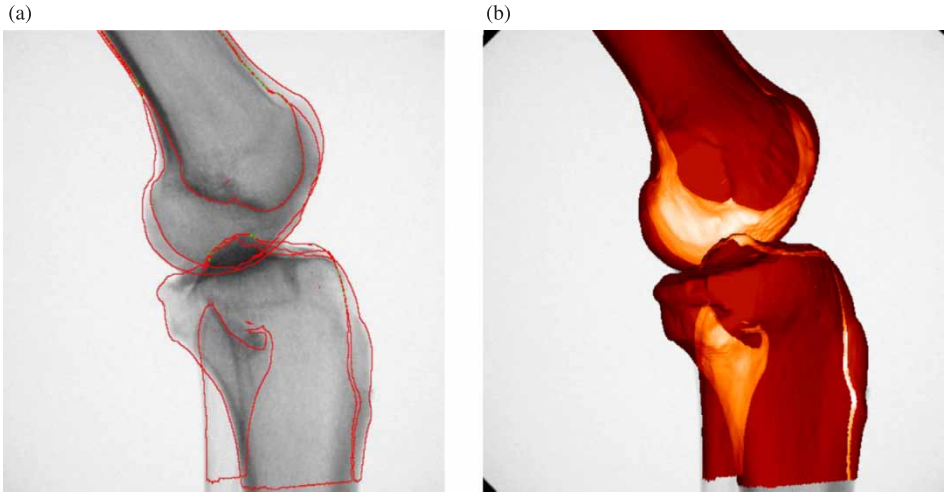

Figure 4. (a) Diagram illustrating how a bone contour was aligned to a fluoroscopy image in this study. (b) The 3D geometry of the femur and tibia superimposed onto a fluoroscopic image.

assumption for cartilage, as during short-time loadings the cartilage continuum deforms without change in volume and behaves like an incompressible elastic solid (Armstrong *et al.* 1984). For longer time loadings, where the viscoelastic behaviour of cartilage is important than more complex models may be employed such as the biphasic (solid matrix and interstitial fluid) model (Armstrong *et al.* 1984).

The net torques exerted about the ankle, knee, and hip during the step-up task were found by solving an inverse dynamics problem using custom code written in Matlab® (The Mathworks Inc.). The joint torques were decomposed into individual muscle forces by solving a static optimization problem that minimized the sum of the squares of all muscle activations in the model (Crowninshield and Brand 1981). The optimization problem was solved subject to the bounds imposed by the force-length and force-velocity properties of the muscles.

The quadriceps forces calculated from the musculoskeletal model and the tibiofemoral kinematics measured from fluoroscopy were input into a FE model of the patellofemoral joint to determine patellar kinematics and patellofemoral joint forces and pressures. In this model, the patella was constrained by the actions of the patellar tendon and the quadriceps muscles, and by articular contact with the femur.

This surface contact is defined by numerical constraints (interpreted as springs with a penalty stiffness) placed between the patella and femur surfaces to ensure that, the predicted patella position could not penetrate the femur surface. The surface STL meshes used to described the shapes of the distal femur, proximal tibia, and patella were imported into a FE grid generation software called TrueGrid (XYZ Scientific Applications, Inc., CA, USA), and used to create a structured hexahedral mesh. A block mesh that represented the outlines of the bones and cartilage was created, and the surfaces were then projected onto the STL mesh. The result was a uniform structured hexahedral mesh with good convergence properties. One benefit of this approach is that, the current mesh can be stored as a template, which can be used to create models for other subjects. Once an appropriate mesh density was determined, the components were exported to a FE software package (Abaqus, Inc., RI, USA) for assembly (figure 5).

The FE problem was solved using a quasi-static solution method with the bones modelled as rigid shells and the cartilage as deformable volumes. The cartilage and bone interface nodes had their translational and rotational degrees of freedom coupled. An augmented Lagrangian contact method was chosen with a "hard-contact" constraint to ensure no cartilage overlap for patellofemoral contact. The solution took 20 min to run on a PC over 30 steps and predicted patellar kinematics, cartilage contact forces and areas, patellar tendon force and patellofemoral pressure patterns.

3. Results

The accuracy of the pose-estimation procedure used in this study was comparable to that reported in previous studies (Fregly *et al.* 2005a) (table 1). In-plane rotations were estimated to less than 1° and in-plane translations were estimated to be 1–2 mm. The accuracy with which, out-of-plane translations and rotations were estimated was also promising. The procedure was capable of producing out-of-plane rotational accuracy of less than 2°(1.88°),

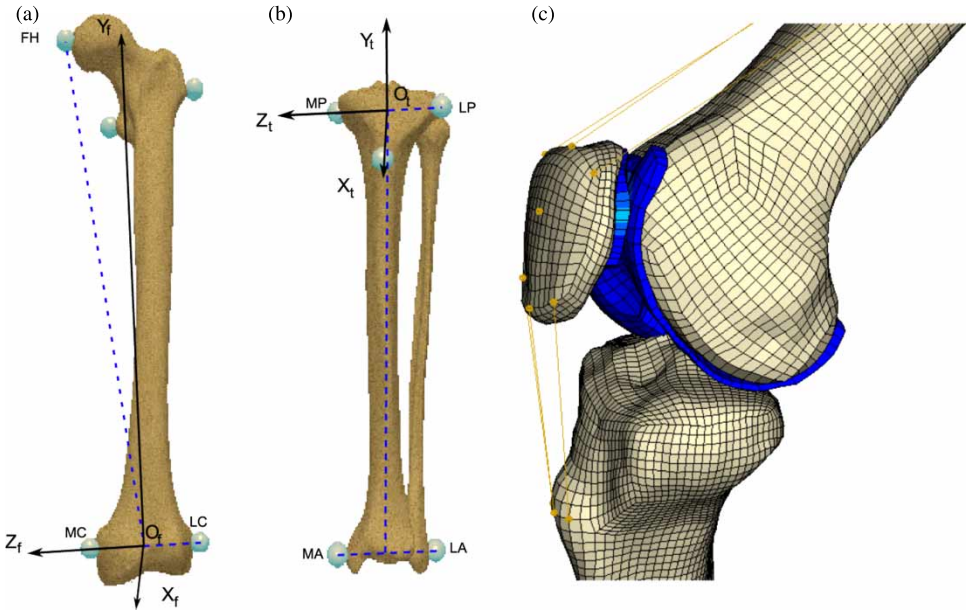

Figure 5. (a) Definition of femur coordinate system where X_f is the femur abduction/adduction axis directed anteriorly, Y_f is the femur rotation axis directed proximally, and Z_f is the femur flexion/extension axis directed medially. (b) Definition of tibia coordinate system where X_t is the tibia abduction/adduction axis directed anteriorly, Y_t is the tibia rotation axis directed proximally, and Z_t is tibia flexion/extension directed medially. (c) Resulting finite element mesh of the knee in Abaqus with attached cartilage, patella tendon and muscle line of action.

Table 1. Accuracy of the pose-estimation procedure used in this study. Tibiofemoral kinematics was estimated using a Vicon motion capture system and a Philips Pulsera Fluoroscopy unit. The results obtained from the Vicon system are regarded as the "gold standard".

	Inplane		Out-of-plane			Inplane
	X (mm) Ant/pos	*Y* (mm) Sup/inf	*Z* (mm) Med/lat	*X* (°) Abduction	*Y* (°) Rotation	*Z* (°) Flexion
Vicon	8.89	38.53	−3.96	6.12	−20.57	−36.39
Philips	6.89	39.56	−7.77	7.99	−20.33	−37.37
Error	2.00	1.03	3.81	1.88	0.24	0.98

which was in agreement with previous studies (Fregly *et al.* 2005a). As expected, the out-of-plane translation was the least accurate of all (3.81 mm), but, was still consistent with other single-plane studies in the literature reporting errors of up to 5.6 mm (Fregly *et al.* 2005a), and can be improved even further by using a biplane system.

The tibiofemoral rotations predicted by the KneeTrack software are reported with respect to the femur. During the extension movement (60–8° of flexion, figure 6A) the tibia adducts (figure 6B) by 4° and rotates externally (figure 6C) by 16°. The tibiofemoral translations are reported with respect to the tibia due to the KneeTrack

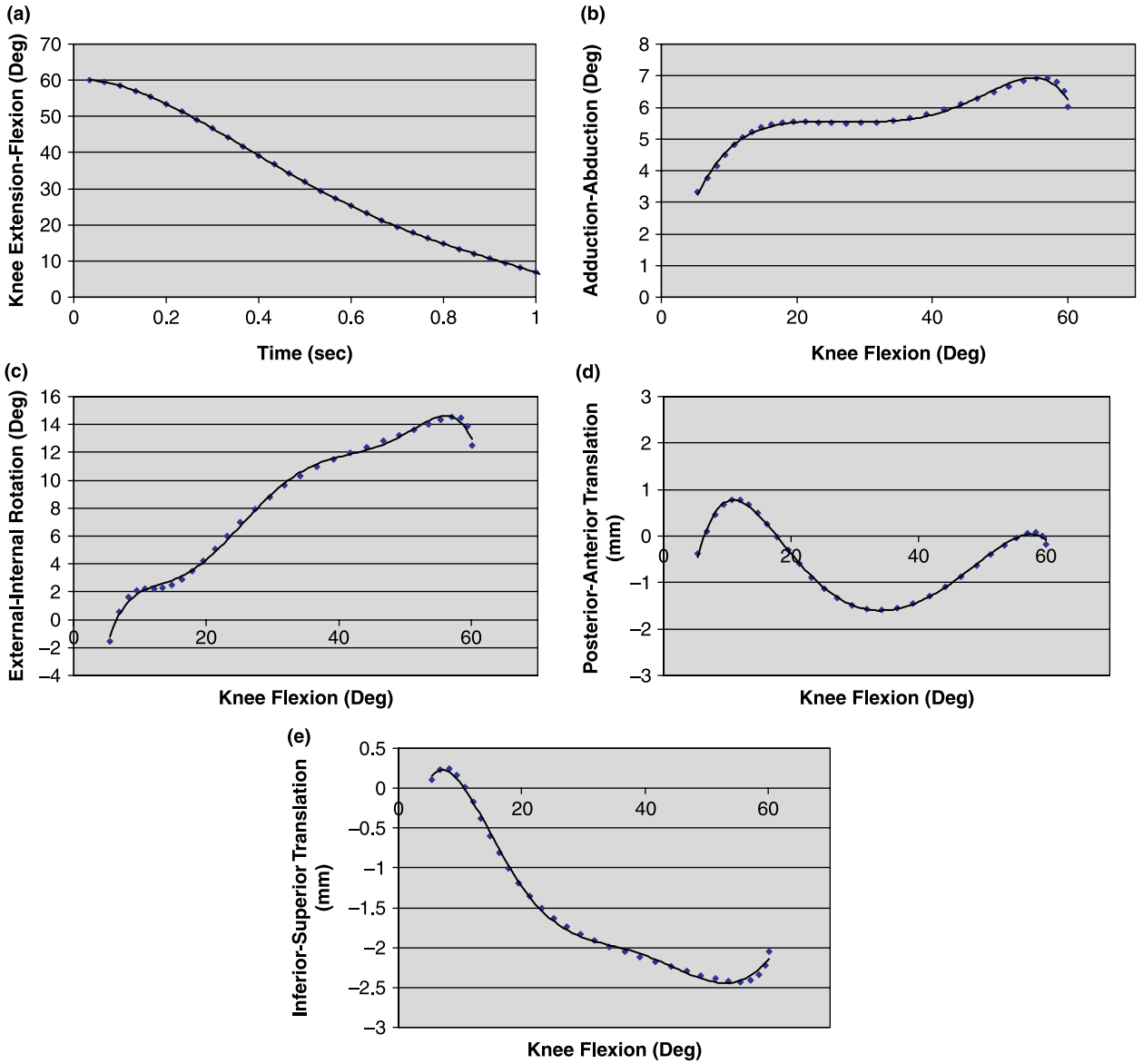

Figure 6. (a) Flexion(+)/extension(−), (b) abduction(+)/adduction(−), (c) Internal(+)/external(−) rotation, (d) anterior(+)/posterior(−) translation and (e) superior(+)/inferior(−) translation kinematics from the KneeTrack software. Note that rotations are reported as tibia movements with respect to the femur and translations are reported as femur movements with respect to the tibia (KneeTrack software convention).

software convention. During extension, the femur moves posterior then anterior over a range of 2 mm, and superiorly (upwards) by 2.5 mm. Most fluoroscopic studies in the literature are for total knee replacements (TKR), hence, only a few studies have reported fluoroscopic results for the natural knee, while other studies have reported kinematics based upon using bone-pins. Some of these studies are used here for comparative purposes.

The range of anterior–posterior translation is very small (~2 mm) when compared to other studies, which used bone pins (Lafortune *et al.* 1992) and X-ray fluoroscopy (DeFrate *et al.* 2004, Dennis *et al.* 2005). This is most likely explained by the flexion axis being defined by fitting two co-axial cylinders to the femoral condyles, and placing the origin of the coordinate system on this axis. This approach has been reported to achieve a more anatomical representation of the actual flexion axis (Eckhoff *et al.* 2005) therefore, this may lead to smaller anterior-posterior translations. The superior translation of the femur with respect to the tibia during the extension movement is in contrast to the trends reported in the literature (Lafortune *et al.* 1992, Benoit *et al.* 2006) for walking studies. This is possibly explained by the fact that, the subject's knee was under high compressive load when in deep flexion at the beginning of the movement, and as the knee extended the compressive load was released resulting in a slight (~2.5 mm) superior movement of the femur with respect to tibia. The range of internal–external motion of about 16° was similar to the results reported by Lafortune *et al.* (1992) and Li *et al.* (2004) (~15°) for the same range of flexion movement. Abduction/adduction values during knee flexion vary greatly in the literature and are therefore, difficult to compare with (Lafortune *et al.* 1992, Benoit *et al.* 2006). The predicted adduction movement of about 4° during knee extension was similar to the results reported by Lafortune *et al.* (1992), but in contrast to the study by Benoit *et al.* (2006).

The net knee extensor torque calculated in the model was similar to values reported in the literature. For example, Vaughan (1996) reported a similar knee-extensor torque trend for the step-up task, where their study included a similar step height, subject weight and subject leg-length to our study (figure 7A). Our peak extensor torque was 90 Nm compared to their value of 65 ± 15 Nm, the difference possibly due to our step length being nearly three times theirs (24 –69 cm). The resultant force developed by the quadriceps muscles decreased as the knee extended from 60 to 8° of flexion (figure 7B). For the period captured by the X-ray, the peak quadriceps force occurred at 60° of knee flexion and was around 2700 N (figure 7B). The increase in quadriceps force corresponded with an increase in contact area between the patella and femur cartilage (figure 8A). The contact area ranged from 75 mm^2 at full extension to 350 mm^2 at 60° flexion in order to keep cartilage pressure low under a higher quadriceps loading. Practically all of the patello-femoral contact force was due to the pull of the quadriceps (figure 8B). The ratios of patellar tendon force to quadriceps force (figure 8C) and patellofemoral contact force to quadriceps force (figure 8D) are also reported and are often used to validate a computer model. Over 60° of knee flexion, the ligament-force/quadriceps-force ratio typically ranges from 1 to 0.7, and the contact-force/quadriceps-force ratio is usually in the range of 0.6–1 as highlighted by others (Huberti *et al.* 1984, Buff *et al.* 1988, Cheng *et al.* 1995, Shelburne and Pandy 1997). The model predicted curves (Figure 8C and D) vary no more than one unit in magnitude from the literature and these differences can be attributed to the use of different subject geometries and muscle insertion locations.

The movements of the patella predicted by the model were consistent with results reported previously by others (Fernandez and Hunter 2005). The patellar coordinate system was based on that previously published by Fernandez and Hunter (2005), where patellar flexion was about the femur flexion axis, patellar tilt was about a longitudinal axis through the superior–inferior poles of the patella, and patellar rotation was about a floating axis directed in an anterior–posterior direction located at the centre of the patella. In general, patellar flexion lagged knee flexion slightly (figure 9A). During knee extension, the patella tilted internally by 10°, rotated internally by 10°, and shifted medially by 4 mm during the step-up task (figure 9B–D). Snapshots of the contact pressure patterns

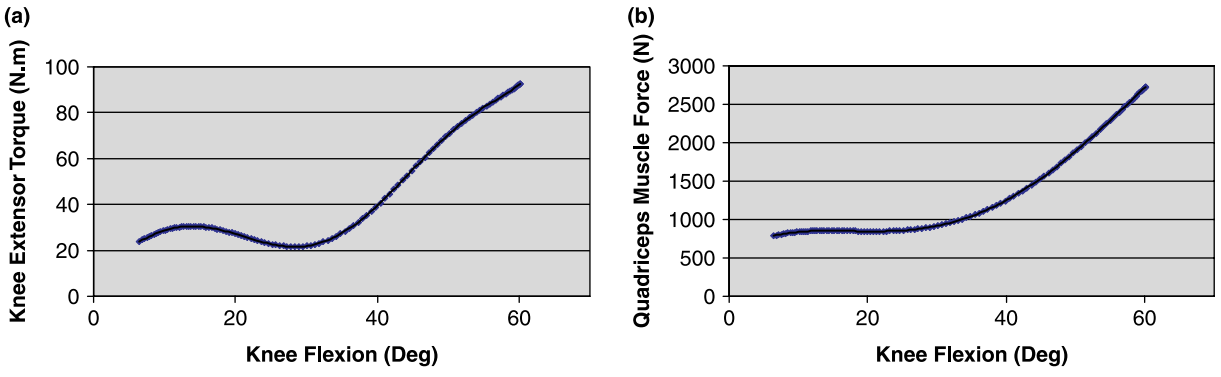

Figure 7. (A) Knee extensor torque calculated for the step-up task; and (B) resultant quadriceps muscle force obtained from static optimization.

calculated in the model are shown for 60, 40 and 15° of knee flexion (figure 10). The contact pattern started with a "figure eight" pattern at 60° flexion and moved distally as the knee extended. The contact pattern was also more prominent on the larger lateral side of the patella, which bears most of the load. Interestingly, the lateral side of the patella is most commonly associated with patellofemoral osteoarthritis. The peak contact pressures calculated in the model were in the range 5–10 MPa, which is consistent with results obtained by others (Besier *et al.* 2005, Fernandez and Hunter 2005).

4. Discussion

There have been numerous finite-element models of the patellofemoral joint presented in the literature. A few studies have also quantified relative movements of the femur, tibia, and patella using single-plane fluoroscopy. However, efforts to integrate these tools in a modelling framework have been scarce, and, to the author's knowledge, using X-ray fluoroscopy to drive a model of the patellofemoral joint is new. The following areas of improvement represent future objectives to make this tool useful in a clinical setting.

A primary objective of our model is to make it patient-specific. While the bone and cartilage geometry, ground reaction forces, joint kinematics and net torques used to drive the model are subject-specific, the moment arms were taken from a generic model, which means that the calculations of quadriceps loading are, to some extent, subject independent. Since, MRI is already an explicit part of the modelling process, it is possible to record musculoskeletal geometry (i.e. muscle moment arms) on a subject-specific basis. These moment arm measurements, along with subject-specific anthropometry, could be used to scale and customise the generic moment arms that are presently calculated in the lower-limb model.

In this study, the joint kinematic measurements derived from the Vicon system and its associated inverse dynamics software to estimate the net extensor torque at the knee during the step-up task were used. Although the more accurate kinematic measurements obtained from X-ray fluoroscopy could have been used to estimate the knee-joint torque, it was not necessary to do so, because quadriceps force was calculated using a model that represented the knee as a hinge (Anderson and Pandy 2001b). The use of a hinge to represent a knee when calculating quadriceps muscle forces should not be too different from a model that uses 6 degrees of freedom at the knee as the primary movement for this study is an extension task. Further, using a whole-body model to calculate muscle forces will always require the use of skin-mounted markers, since all joints (e.g., ankle, knee, hip and upper limb) cannot be captured simultaneously using X-ray fluoroscopy. In future studies, we propose to couple the Vicon and X-ray kinematic data into a neuromuscular "tracking" (NMT) method (Seth and

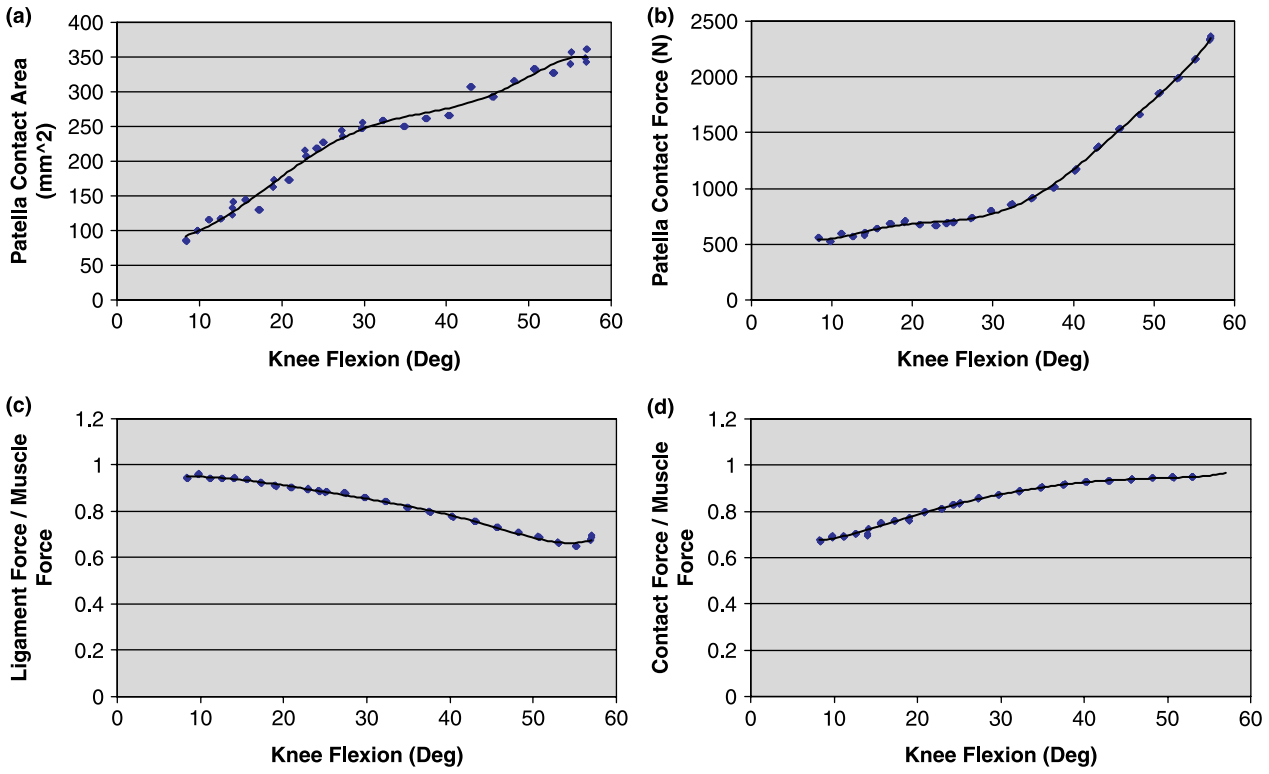

Figure 8. Patella-femoral model prediction of (A) contact area, (B) contact force, (C) ratio of patellar tendon force to quadriceps force, and (D) ratio of patellofemoral contact force to quadriceps force.

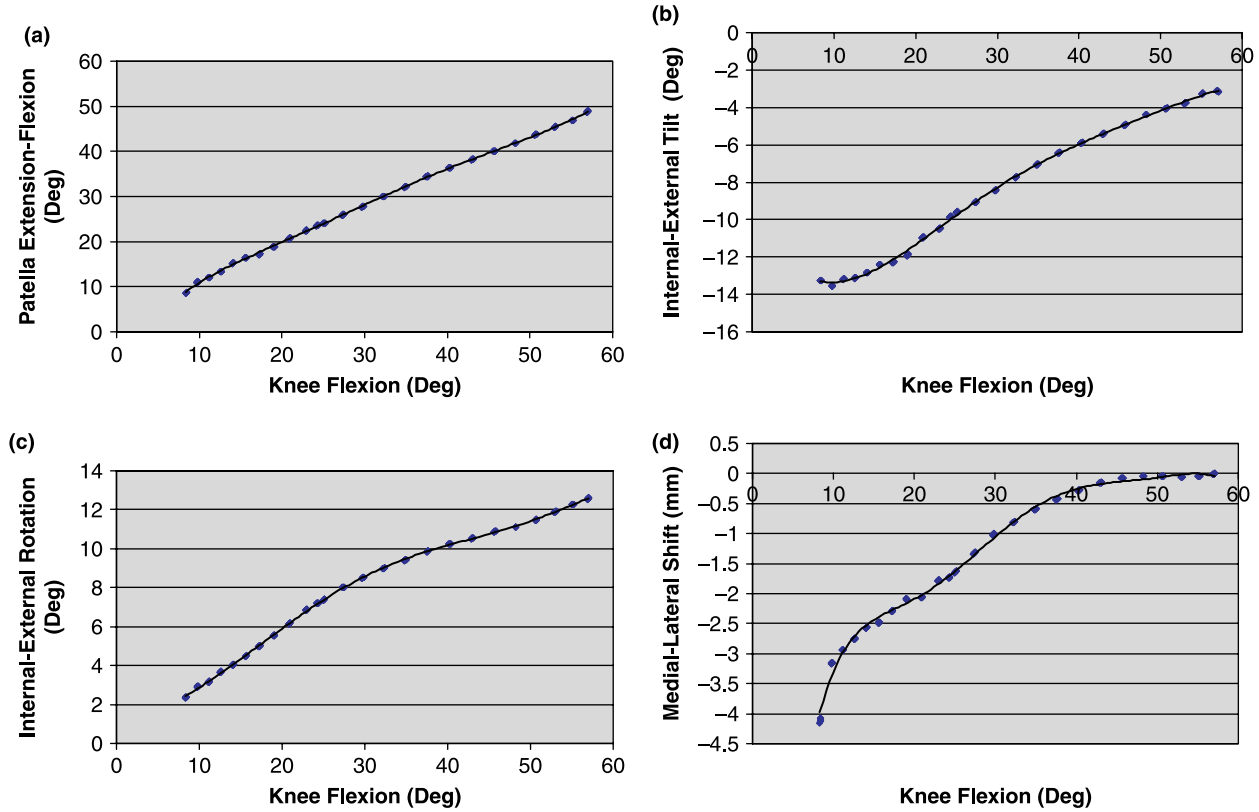

Figure 9. Movement of the patella relative to the femur as calculated by the FE patellofemoral model. Patella (a) flexion(+)/extension(−); (b) external(+)/internal(−) tilt; (c) external(+)/internal(−) rotation; and (d) lateral(+)/medial(−) translation (patellar shift).

Pandy 2006), so that forward simulations of knee-joint motion can be performed during dynamic activity. The NMT method has been used to track ground-reaction forces and joint kinematics in tasks such as vertical jumping and gait. One advantage of NMT over other tracking methods is that it includes muscle activation dynamics in the formulation of the optimization problem.

While sub-millimetre translation errors have been presented in the literature for both single and biplane fluoroscopy, these error estimates vary greatly, and some features of the pose-estimation process are even neglected in the error analysis. To gain confidence in the estimated measurement error, analyses must be performed that propagate the error from the image segmentation stage (for feature-based methods) all the way through to the final stage of calculating the joint translations and rotations. For example, there are a number of errors associated with the image processing procedures alone. First, although MRI can provide information on fine anatomical detail such as cartilage volume, a significant amount of user intervention is needed to differentiate bone from the soft tissue, which introduces operator dependent error. Second, MRI has known geometric distortion effects (Wang *et al.* 2004), which can be highlighted by developing the same model geometry using CT. Third, the X-ray focal spot (i.e. the area on the X-ray tube anode that the electrons strike), which is related to the image resolution, should be the starting point for setting the minimum resolution that can be detected. Further work is needed to quantify the errors associated with these separate processes before pose-estimation can be used as a clinical tool.

The accuracy of fluoroscopic methods is usually established by performing a validation study. In this study, we performed a static validation test using dry cadaver bones. Perhaps the most serious limitation of the results given in table 1 is that they may not be applicable to dynamic motion. Previous validation studies reported in the literature have employed various techniques to quantify the errors associated with fluoroscopic measurements. One study measured the relative orientation and distance between two non-anatomical (ball and cylinder) objects (Li *et al.* 2004). Another study, (Komistek *et al.* 2003) used implants that were moved into known orientations by a test rig, with noise added to resemble soft tissue movement relative to the underlying bones. Human cadavers and optical sensors have also been used to measure knee kinematics over the full range of motion of the joint (Komistek *et al.* 2003). The measurement errors obtained in all of these studies were roughly comparable-less than 0.5 mm for joint translations and less than 0.5 for joint rotations. Our future work will include a more thorough validation study that takes into account the actual *in vivo* testing conditions, image processing issues and the dynamic conditions of the task being modelled.

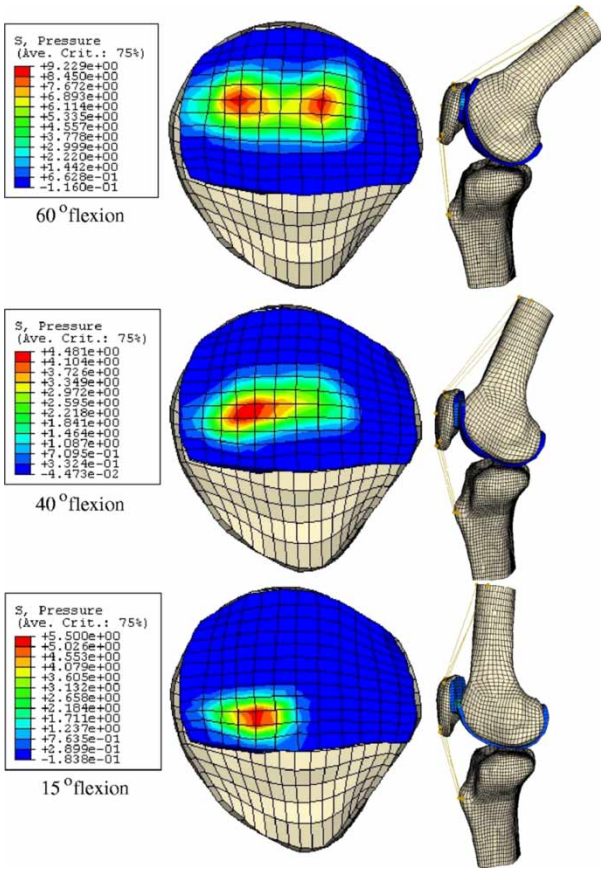

Figure 10. Patella surface stress in MPa and pressure patterns for 60, 40 and 15° of knee flexion. Also shown on the right are the corresponding positions of the bones in the model.

The main aim of this paper was to illustrate how X-ray fluoroscopy, motion capture and computational modelling can be integrated for the purpose of assessing patellofemoral function during dynamic activity. The calculations obtained from the model were qualitatively compared with results reported in the literature. The next step is to use the model to simulate a number of other tasks, such as squatting, level walking, stair rise and stair descent. It will be necessary to validate the model against measurements made for these tasks as well, before the model can be used with confidence to make predictions about muscle and joint function in pathologies such as patellofemoral osteoarthritis. Application of our modelling framework to the natural knee may enable patients suffering from osteoarthritis to be diagnosed earlier. Other uses of the modelling framework described in this paper include (a) evaluating the performance of joint replacements *in vivo* during normal weight-bearing activities, so that engineers are then able to improve on current designs; (b) aiding in the design of better tissue-engineered constructs for cartilage replacement, and (c) helping physiotherapists to design more effective exercise-based muscle-strengthening programs for treatment of joint pain caused by osteoarthritis.

Finally, some examples of how our patellofemoral model may be used to study specific clinical problems include simulating the effects of patellar maltracking, cartilage thinning, joint stiffening and joint incongruency, all of which are known to lead to the occurrence of patellofemoral osteoarthritis. The model may also be used to simulate the effects of corrective surgeries, such as a vastus lateralis release. In this procedure, a portion of the vastus lateralis tendon is released via keyhole surgery to reduce the pressure on the lateral side, which is believed to be the cause of anterior knee pain and cartilage degeneration (Aderinto and Cobb 2002). The benefits of a FE model of the patella over rigid-body models include the ability to model internal cartilage and bone stresses that can lead to crack growth, and testing improved constitutive laws for cartilage tissue. The model can also be extended to a dynamic explicit formulation that allows very fast movements, such as running and jumping, to be simulated with high fidelity (provided a higher frame rate is used when recording knee kinematics using X-ray fluoroscopy).

Acknowledgements

We thank Dr Scott Banks, University of Florida, for allowing the KneeTrack software to be used in this project. We also gratefully acknowledge Prof. Brian Tress, Mr Ronnie Li and Dr Paul Einsiedel of The Royal Melbourne Hospital for their help with the X-ray fluoroscopy data collection. Finally, we thank Assoc. Prof. Chris Briggs, University of Melbourne, and Assoc. Prof. Martin Richardson, The Royal Melbourne Hospital, for donation of the dry cadaver bones and bone cement and Mr Tam Nguyen for his help with the inverse dynamics analysis.

References

J. Aderinto and A.G. Cobb, "Lateral release for patellofemoral arthritis", *Arthroscopy*, 18, pp. 399–403, 2002.

E.J. Alexander and T.P. Andriacchi, "Improving the analysis of human movement using markerless motion capture", Bioengineering Conference, June 25–29, Sonesta Beach Resort in Key Biscayne, Florida, 2003.

F.C. Anderson and M.G. Pandy, "Dynamic optimization of human walking", *J. Biomech. Eng.*, 123, pp. 381–390, 2001a.

F.C. Anderson and M.G. Pandy, "Static and dynamic optimization solutions for gait are practically equivalent", *J. Biomech.*, 34, pp. 153–161, 2001b.

T.P. Andriacchi, E. Alexander, M. Toney, C. Dyrby and J. Sum, "A point cluster technique for *in vivo* motion analysis: applied to a study of knee kinematics", *J. Biomech. Eng.*, 120, pp. 743–749, 1998.

C.G. Armstrong, W.M. Lai and V.C. Mow, "An analysis of the unconfined compression of articular cartilage", *J. Biomech. Eng.*, 106, pp. 165–173, 1984.

ARPANSA, *ARPANSA-Radiation Protection Series Publication No. 8 (RPS-8)* Exposure of Humans to Ionizing Radiation for Research Purposes, 2005.

D.S. Asakawa, K.S. Nayak, S.S. Blemker, S.L. Delp, J.M. Pauly, D.G. Nishimura and G.E. Gold, "Real-time imaging of skeletal muscle velocity", *J. Magn. Reson. Imaging*, 18, pp. 734–739, 2003.

S.A. Banks and W.A. Hodge, "Accurate measurement of three-dimensional knee replacement kinematics using single-plane fluoroscopy", *IEEE Trans. Biomed. Eng.*, 43, pp. 638–649, 1996.

P. Beillas, G. Papaioannou, S. Tashman and K.H. Yang, "A new method to investigate *in vivo* knee behavior using a finite element model of the lower limb", *J. Biomech.*, 37, pp. 1019–1030, 2004.

D.L. Benoit, D.K. Ramsey, M. Lamontagne, L. Xu, P. Wretenberg and P. Renstrom, "Effect of skin movement artifact on knee kinematics during gait and cutting motions measured *in vivo*", *Gait Posture*, 24, pp. 152–164, 2006.

T.F. Besier, G.E. Gold, G.S. Beaupre and S.L. Delp, "A modeling framework to estimate patellofemoral joint cartilage stress *in vivo*", *Med. Sci. Sports Exerc.*, 37, pp. 1924–1930, 2005.

H. Buff, L. Jones and D. Hungerford, "Experimental determination of forces transmitted through the patello-femoral joint", *J. Biomech.*, 21, pp. 17–23, 1988.

A. Cappello, R. Stagni, S. Fantozzi and A. Leardini, "Soft tissue artifact compensation in knee kinematics by double anatomical landmark calibration: performance of a novel method during selected motor tasks", *IEEE Trans. Biomed. Eng.*, 52, pp. 992–998, 2005.

C.K. Cheng, N.K. Yao and H.C. Liu, "Surgery simulation analysis of anterior advancement of the tibial tuberosity", *Clin. Biomech.*, 10, pp. 115–121, 1995.

R. Crowninshield and R. Brand, "A physiologically based criterion of muscle force prediction in locomotion", *J. Biomech.*, 14, pp. 793–801, 1981.

L.E. DeFrate, H. Sun, T.J. Gill, H.E. Rubash and G. Li, "*In vivo* tibiofemoral contact analysis using 3D MRI-based knee models", *J. Biomech.*, 37, pp. 1499–1504, 2004.

D.A. Dennis, M.R. Mahfouz, R.D. Komistek and W. Hoff, "*In vivo* determination of normal and anterior cruciate ligament-deficient knee kinematics", *J. Biomech. Knee Mech.*, Updat. Theor. Exp. Anal. 38, pp. 241–253, 2005.

D.G. Eckhoff, J.M. Bach, V.M. Spitzer, K.D. Reinig, M.M. Bagur, T.H. Baldini and N.M.P. Flannery, "Three-Dimensional mechanics, kinematics, and morphology of the knee viewed in virtual reality", *J. Bone Joint Surg.*, 87, pp. 71–80, 2005.

J.W. Fernandez and P.J. Hunter, "An anatomically based patient-specific finite element model of patella articulation: towards a diagnostic tool", *Biomech. Model. Mechanobiol.*, 4, pp. 20–38, 2005.

B.J. Fregly, H.A. Rahman and S.A. Banks, "Theoretical accuracy of model-based shape matching for measuring natural knee kinematics with single-plane fluoroscopy", *J. Biomech. Eng.*, 127, pp. 692–699, 2005a.

B.J. Fregly, W.G. Sawyer, M.K. Harman and S.A. Banks, "Computational wear prediction of a total knee replacement from *in vivo* kinematics", *J. Biomech.*, 38, pp. 305–314, 2005b.

J. Fuller, L.-J. Liu, M.C. Murphy and R.W. Mann, "A comparison of lower-extremity skeletal kinematics measured using skin- and pin-mounted markers", *Hum. Mov. Sci.*, 16, pp. 219–242, 1997.

A.C. Godest, C.S. de Cloke, M. Taylor, P.J. Gregson, A.J. Keane, S. Sathasivan and P.S. Walker, "A computational model for the prediction of total knee replacement kinematics in the sagittal plane", *J. Biomech.*, 33, pp. 435–442, 2000.

A.C. Godest, M. Beaugonin, E. Haug, M. Taylor and P.J. Gregson, "Simulation of a knee joint replacement during a gait cycle using explicit finite element analysis", *J. Biomech.*, 35, pp. 267–275, 2002.

J.P. Halloran, A.J. Petrella and P.J. Rullkoetter, "Explicit finite element modeling of total knee replacement mechanics", *J. Biomech. Knee Mech.*, Updat. Theor. Exp. Anal. 38, pp. 323–331, 2005.

J. Heegaard, P.F. Leyvraz, A. Curnier, L. Rakotomanana and R. Huiskes, "The biomechanics of the human patella during passive knee flexion", *J. Biomech.*, 28, pp. 1265–1279, 1995.

J.H. Heegaard, P.F. Leyvraz and C.B. Hovey, "A computer model to simulate patellar biomechanics following total knee replacement: the effects of femoral component alignment", *Clin. Biomech.*, (Bristol, Avon) 16, pp. 415–423, 2001.

W.A. Hoff, R.D. Komistek, D.A. Dennis, S.M. Gabriel and S.A. Walker, "Three-dimensional determination of femoral-tibial contact positions under *in vivo* conditions using fluoroscopy", *Clin. Biomech.*, 13, pp. 455–472, 1998.

H. Huberti, W. Hayes, J. Stone and G. Shybut, "Force ratios in the quadriceps tendon and ligamentum patellae", *J. Orthop. Res.*, 2, pp. 49–54, 1984.

J.-i. Ishikawa, G.L. Niebur, S. Uchiyama, R.L. Linscheid, A. Minami, K. Kaneda and K.-N. An, "Feasibility of using a magnetic tracking device for measuring carpal kinematics", *J. Biomech.*, 30, pp. 1183–1186, 1997.

J. Karrholm, "Roentgen stereophtogrammetry", Review of Orthopedic Applications *Acta Orthop. Scand.*, 60, pp. 491–503, 1989.

R.D. Komistek, D.A. Dennis and M.R. Mahfouz, "*In vivo* fluoroscopic analysis of the normal human knee", *Clin. Orthop.*, 410, pp. 69–81, 2003.

M.A. Lafortune, P.R. Cavanagh, I. Sommer, J. H and A. Kalenak, "Three-dimensional kinematics of the human knee during walking", *J. Biomech.*, 25, pp. 347–357, 1992.

J. Laprade and R. Lee, "Real-time measurement of patellofemoral kinematics in asymptomatic subjects", *Knee*, 12, pp. 63–72, 2005.

G. Li, T.H. Wuerz and L.E. DeFrate, "Feasibility of using orthogonal fluoroscopic images to measure *in vivo* joint kinematics", *J. Biomech. Eng.*, 126, pp. 313–318, 2004.

Z.-P. Luo, G.K. Niebur and K.-N. An, "Determination of the proximity tolerance for measurement of surface contact areas using a magnetic tracking device", *J. Biomech.*, 29, pp. 367–372, 1996.

M.R. Mahfouz, W.A. Hoff, R.D. Komistek and D.A. Dennis, "Effect of segmentation errors on 3D-to-2D registration of implant models in X-ray images", *J. Biomech. Knee Mech.*, Updat. Theor. Exp. Anal. 38, pp. 229–239, 2005.

J. McConville, T.D. Churchil III, I. Kaleps, C. Clauser and J. Cuzzi, *Anthropometric Relationships of Body and Body Segment Moments of Inertia*, Rep. AFAMRL-TR-80-119, Wright-Patterson Air Force Base, 1980.

A.D. Milne, D.G. Chess, J.A. Johnson and G.J.W. King, "Accuracy of an electromagnetic tracking device: a study of the optimal operating range and metal interference", *J. Biomech.*, 29, pp. 791–793, 1996.

L. Mundermann, S. Corazza and T. Andriacchi, "The evolution of methods for the capture of human movement leading to markerless motion capture for biomechanical applications", *J. NeuroEng. Rehabil.*, 3, p. 6, 2006.

V.V. Patel, K. Hall, M. Ries, C. Lindsey, E. Ozhinsky, Y. Lu and S. Majumdar, "Magnetic resonance imaging of patellofemoral kinematics with weight-bearing", *J. Bone Joint Surg. Am.*, 85, pp. 2419–2424, 2003.

G.P. Penney, J. Weese, J.A. Little, P. Desmedt, D.L.G. Hill and D.J. Hawkes, "A comparison of similarity measures for use in 2-D-3-D medical image registration", *IEEE Trans. Med. Imaging*, 17, pp. 586–595, 1998.

W.A. Scott Tashman, "*In vivo* measurement of dynamic joint motion using high speed biplane radiography and CT: application to canine ACL deficiency", *J. Biomech. Eng.*, 125, pp. 238–245, 2003.

A. Seth and M.G. Pandy, "A neuromusculoskeletal tracking method for estimating individual muscle forces in human movement", *J. Biomech.*, 2006.

F.T. Sheehan, F.E. Zajac and J.E. Drace, "*In vivo* tracking of the human patella using cine phase contrast magnetic resonance imaging", *J. Biomech. Eng.*, 121, pp. 650–656, 1999.

K. Shelburne and M. Pandy, "A musculoskeletal model of the knee for evaluating ligament forces during isometric contractions", *J. Biomech.*, 30, pp. 163–176, 1997.

F.G. Shellock and J.V. Crues, "MR procedures: biologic effects, safety, and patient care", *Radiology*, 232, pp. 635–652, 2004.

R. Stagni, S. Fantozzi, A. Cappello and A. Leardini, "Quantification of soft tissue artefact in motion analysis by combining 3D fluoroscopy and stereophotogrammetry: a study on two subjects", *Clin. Biomech.*, 20, pp. 320–329, 2005.

M.A. Taiyo Asano, K. Tanaka, J. Tamura and T. Nakamura, "*In vivo* three-dimensional knee kinematics using a biplanar image-matching technique", *Clin. Orthop.*, 388, pp. 157–166, 2001.

M.A. Taiyo Asano, K. Koike and T. Nakamura, "*In vivo* three-dimensional patellar tracking", *Clin. Orthop.*, 413, pp. 222–232, 2003.

E.R. Valstar, "Digital Roentgen stereophotogrammetry: development, validation, and clinical application", In: Department of Orthopaedics. Leiden University, 2001.

C.L. Vaughan, "Are joint torques the Holy Grail of human gait analysis?", *Hum. Mov. Sci.*, 15, pp. 423–443, 1996.

D. Wang, W. Strugnell, G. Cowin, D.M. Doddrell and R. Slaughter, "Geometric distortion in clinical MRI systems Part I: evaluation using a 3D phantom", *Magn. Reson. Imaging*, 22, pp. 1211–1221, 2004.

T. Yamazaki, T. Watanabe, Y. Nakajima, K. Sugamoto, T. Tomita, D. Maeda, W. Sahara, H. Yoshikawa and S. Tamura, "Visualization of femorotibial contact in total knee arthroplasty using X-ray

fluoroscopy", *Eur. J. Radiol. Pediatr. Intervent. Angiography*, 53, pp. 84–89, 2005.

B.-M. You, P. Siy, W. Anderst and S. Tashman, "*In vivo* measurement of 3-D skeletal kinematics from sequences of biplane radiographs: application to knee kinematics", *IEEE Trans. Med. Imaging*, 20, pp. 514–525, 2001.

X. Yuan, L. Ryd, K.E. Tanner and L. Lidgren, "Roentgen single-plane photogrammetric analysis (RSPA): a new approach to the study of musculoskeletal movement", *J. Bone Joint Surg. Br.*, 84, pp. 908–914, 2002.

F. Zajac, "Muscle and tendon: properties, models, scaling, and application to biomechanics and motor control", *Crit. Rev. Biomed. Eng.*, 17, pp. 359–411, 1989.

S. Zuffi, A. Leardini, F. Catani, S. Fantozzi and A. Cappello, "A model-based method for the reconstruction of total knee replacement kinematics", *IEEE Trans. Med. Imaging*, 18, pp. 981–991, 1999.